Breast Cancer Research and Treatment (2019) 178:75–86
https://doi.org/10.1007/s10549-019-05376-9

PRECLINICAL STUDY

# PK-M2-mediated metabolic changes in breast cancer cells induced by ionizing radiation

**Le Zhang[1] · Justine Bailleul[1] · Taha Yazal[1] · Kevin Dong[1] · David Sung[1] · Amy Dao[1] · Laura Gosa[2] · David Nathanson[2,3] · Kruttika Bhat[1] · Sara Duhachek-Muggy[1] · Claudia Alli[1] · Milana Bochkur Dratver[1] · Frank Pajonk[1,3] · Erina Vlashi[1,3]**

Received: 2 March 2019 / Accepted: 23 July 2019 / Published online: 1 August 2019


## Abstract

**Purpose** Radiotherapy (RT) constitutes an important part of breast cancer treatment. However, triple negative breast cancers (TNBC) exhibit remarkable resistance to most therapies, including RT. Developing new ways to radiosensitize TNBC cells could result in improved patient outcomes. The M2 isoform of pyruvate kinase (PK-M2) is believed to be responsible for the re-wiring of cancer cell metabolism after oxidative stress. The aim of the study was to determine the effect of ionizing radiation (IR) on PK-M2-mediated metabolic changes in TNBC cells, and their survival. In addition, we determine the effect of PK-M2 activators on breast cancer stem cells, a radioresistant subpopulation of breast cancer stem cells.

**Methods** Glucose uptake, lactate production, and glutamine consumption were assessed. The cellular localization of PK-M2 was evaluated by western blot and confocal microscopy. The small molecule activator of PK-M2, TEPP46, was used to promote its pyruvate kinase function. Finally, effects on cancer stem cell were evaluated via sphere forming capacity.

**Results** Exposure of TNBC cells to IR increased their glucose uptake and lactate production. As expected, PK-M2 expression levels also increased, especially in the nucleus, although overall pyruvate kinase activity was decreased. PK-M2 nuclear localization was shown to be associated with breast cancer stem cells, and activation of PK-M2 by TEPP46 depleted this population.

**Conclusions** Radiotherapy can induce metabolic changes in TNBC cells, and these changes seem to be mediated, at least in part by PK-M2. Importantly, our results show that activators of PK-M2 can deplete breast cancer stem cells in vitro. This study supports the idea of combining PK-M2 activators with radiation to enhance the effect of radiotherapy in resistant cancers, such as TNBC.

**Keywords** Pyruvate kinase · Radiation therapy · Breast cancer · Metabolism

Le Zhang and Justine Bailleul have contributed equally to this work.

**Electronic supplementary material** The online version of this article (https://doi.org/10.1007/s10549-019-05376-9) contains supplementary material, which is available to authorized users.

✉ Erina Vlashi
evlashi@mednet.ucla.edu

[1] Department of Radiation Oncology, David Geffen School of Medicine at UCLA, 10833 Le Conte Ave, Los Angeles, CA 90095-1714, USA

[2] Department of Molecular and Medical Pharmacology, David Geffen School of Medicine, University of California, Los Angeles, Los Angeles, CA, USA

[3] Jonsson Comprehensive Cancer Center, University of California, Los Angeles, Los Angeles, CA, USA

## Abbreviations

| | |
|---|---|
| $^{18}$FDG | [$^{18}$F]fluorodeoxyglucose |
| 2NBDG | 2-deoxy-2-[(7-nitro-2,1,3-benzoxadiazol-4-yl) amino]-D-glucose |
| BC | Breast cancer |
| bFGF | Fibroblast growth factor 2 |
| CSC | Cancer stem cell |
| EGF | Epidermal growth factor |
| GAPDH | Glyceraldehyde 3-phosphate dehydrogenase |
| GSH | Glutathione |
| H2DCFA | 2′,7′-dichlorodihydrofluorescein diacetate |
| HIF1α | Hypoxia inducible factor |
| IR | Ionizing radiation |
| NADPH | Nicotinamide adenine dinucleotide phosphate |
| PK-M2 | M2 isoform of pyruvate kinase |
| PPP | Pentose phosphate pathway |

| | |
|---|---|
| ROS | Reactive oxygen species |
| RT | Radiation therapy |
| TNBC | Triple negative breast cancer |

## Introduction

Radiation therapy (RT) is often part of a successful treatment regimen for breast cancer (BC) [1]. However, triple negative breast cancer (TNBC) has a poor prognosis and resists most treatment approaches, including RT [2]. Therapeutic approaches that radiosensitize this subtype of breast cancer could substantially improve the outcome. One reason for resistance to RT [3, 4] is the presence of cells with "stem cell" characteristics (cancer stem cells, CSCs) that escape cytotoxic therapy and cause relapses [5–8].

It is well recognized that ionizing radiation (IR), such as used in RT, exerts its cytotoxic effect mainly through the generation of highly reactive oxygen species (ROS) that damage macromolecules and critical cellular structures [9]. Often cancer cells adapt to oxidative stress as a way of surviving in a harsh tumor microenvironment [10], and metabolic plasticity can facilitate such adaptation. For example, yeast and normal mammalian cells are capable of re-wiring their glucose metabolism in response to oxidative stress and this process involves redox-sensitive enzymes in lower glycolysis, such as glyceraldehyde 3-phosphate dehydrogenase (GAPDH) [11–13]. Cancer cells, however, generally use the last rate-limiting enzyme in glycolysis, the M2 isoform of pyruvate kinase (PK-M2) to reprogram their metabolism during oxidative stress [14].

PK-M2 is overexpressed in a number of cancers, including BC [15–18], where it facilitates the "Warburg effect" by increasing basal levels of glycolysis [17, 19, 20] and its expression correlates with patient survival [18]. PK-M2 is unique from all the other isoforms of pyruvate kinase due to its conformational flexibility. PK-M2 tetramers efficiently convert phosphoenol pyruvate to pyruvate in glycolysis, while PK-M2 dimers are enzymatically inactive—this creates a "bottleneck" in glycolytic flux resulting in rapid accumulation of intermediate metabolites that become available for the upstream pentose phosphate pathway (PPP). Growth factors can inactivate PK-M2 resulting in metabolic reprogramming to meet the anabolic demands of rapidly proliferating cancer cells [21, 22]. However, oxidative stress also inactivates PK-M2, re-directing glucose metabolites into the PPP resulting in increased production of the anti-oxidant NADPH [14] and restoration of the redox state of the cell. The conformational flexibility of PK-M2, therefore, endows cancer cells with metabolic flexibility to meet context-specific metabolic needs [17]. In addition, PK-M2 dimers are often found in the nucleus moonlighting as transcriptional regulators of a number of genes ranging from stem cell pathways to DNA damage repair [23–26]. Importantly, small molecule *activators* of PK-M2 boost oxidative stress and have anti-proliferative activity in cancer cells [14, 27, 28].

Most studies investigating the effect of oxidative stress on cellular metabolism have utilized either chemically-induced oxidative stress (i.e., via $H_2O_2$ or diamide) or hypoxia [11, 13, 14, 29, 30]. There are multiple reasons why the cellular responses to chemically-induced oxidative stress differ from the response to IR and are not directly relevant to RT. Therefore, in the study presented here we have investigated the effect of IR on the metabolism of TNBC, and more specifically on PK-M2 in unselected cells, as well as in radiation-resistant BC stem cells which are metabolically distinct from their more differentiated progeny [31, 32].

## Materials and methods

### Cell culture

Human SUM159PT and MDA-MB-231 breast cancer cell lines were purchased from Asterandt (Detroit, MI) and ATCC respectively. SUM159PT cells were cultured in F12 medium (Thermofisher) supplemented with 5% fetal bovine serum (FBS), penicillin and streptomycin cocktail (Thermofisher), 5 µg/mL insulin (humulin R, Lilly), 10 mM HEPES (Thermofisher), and 1 µg/mL hydrocortisone (Solu-Cortef, Pfizer). SUM159PT-cODC-ZsGreen cells were obtained as previously described [33]. MDA-MB-231 cells were cultured in Dulbecco's Modified Eagle Medium (DMEM) (Thermofisher) supplemented with 20% FBS, and penicillin and streptomycin cocktail. All cells were grown at 37 °C, in a humidified incubator with 5% $CO_2$.

### Irradiation and treatments

Cells were irradiated at room temperature using an experimental X-ray irradiator (Gulmay Medical Inc, Suwanee, GA) at a dose rate of 7.1702 Gy/min. The X-ray beam was operated at 300 kV and hardened using 4-mm Be, 3-mm Al, and 1.5-mm Cu filters. Corresponding controls were sham irradiated. Dosimetry was standardized to NIST using ion chambers and film. Cells were treated with 10 µM TEPP46 (CCKinase, Inc.) [27] 1 h prior to irradiation.

### Mammosphere assay

Mammosphere-forming capacity was performed by plating cells in DMEM/F-12, 0.4% bovine serum albumin (BSA) (VWR), 10 mL/500 mL B27 (Thermofisher) 5 µg/mL insulin, 4 µg/mL heparin (Sagent, Schaumburg, IL), 20 ng/mL fibroblast growth factor 2 (bFGF) (StemCell Technologies), and 20 ng/mL epidermal growth factor (EGF) (StemCell

Technologies) into 96-well ultra-low adhesion plates, at a range of cell densities, with EGF, bFGF, and heparin added every 3 days. The number of spheres formed per well was counted and expressed as a percentage of the initial number of cells plated.

## Clonogenic colony formation assays

SUM159PT and MDA-MB-231 cells were plated as monolayers in serum-supplemented media and treated with vehicle or TEPP46 (10 μM) 24 h after plating. A second treatment was administered to the cells 24 h after the first treatment. Three hours later, cells were detached and counted. Cell suspensions were prepared at the appropriate cell concentration to account for cell toxicity in each irradiation dose (200 cells per well for 0 and 2 Gy for both cell lines; 1600 cells per well for 8 Gy for SUM159PT and 9600 cells for 8 Gy for MDA-MB-231). Cells were irradiated in conical 15 mL tubes right before plating in 6-well tissue culture-treated plates. Triplicate technical repeats were performed for each condition. Cells were incubated at 37 °C with 5% $CO_2$ in a humidified atmosphere. After 10 to 15 days, cells were fixed with 70% ethanol and stained with crystal violet. Colonies with at least 50 cells were counted. The survival fractions were determined by normalizing each irradiated condition to its non-irradiated control.

## Glucose uptake, glutamine consumption, and lactate production assays

$2x10^5$ cells/well were plated in 6-well plates, allowed to adhere overnight, and irradiated the next day. For measuring glucose uptake, the fluorescent glucose analogue 2-deoxy-2-[(7-nitro-2,1,3-benzoxadiazol-4-yl)amino]-D-glucose (2NBDG) was used (Thermofisher). 1, 3, 24, 48, and 72 h after irradiation exposure, cells were removed by trypsinization. Cells were then incubated for 1 h with 200 μM 2NBDG in glucose-free media at 37 °C. After incubation with 2-NBDG, cells were resuspended in PBS, and analyzed by flow cytometry and the geometrical mean fluorescence was determined. Cells were also sorted based on 2NBDG uptake. $2NBDG^{low}$ and $2NBDG^{high}$ populations were collected and plated either for immunofluorescence or mammosphere-forming assay.

For the [$^{18}$F]fluorodeoxyglucose uptake assay, breast cancer cells were plated at $5 \times 10^4$ cells/well on tissue culture-treated 6-well plates and allowed to adhere overnight. The next day cells were exposed to 0 or 8 Gy. After the indicated time points, cells were collected, counted, and cell numbers were adjusted so the same number of cells for each treatment group was resuspended in glucose-free DMEM/F12 media containing [$^{18}$F]FDG (radioactivity 1 μCi/mL). Cells were incubated at 37 °C for 1 h and then washed 3X with ice-cold PBS. The radioactivity of each sample was then measured with a gamma counter and the resulting counts-per-minute (CPM) values were normalized to the appropriate controls (non-irradiated samples).

For determining glutamine consumption and lactate production, media from wells with cells or empty controls was collected at the indicated time points after irradiation, centrifuged at 10,000×*g* for 10 min at 4 °C to remove insoluble components. The media was used to determine glutamine consumption (Glutamine Assay Kit, Abcam, #ab197011) and the amount of lactate produced (Lactate Assay Kit, Bio Vision, #K607-100). The results were normalized to the cell numbers of each group.

## Protein extraction

Whole cell proteins were extracted from cells at various time points after treatments. Briefly, cells were scraped, washed with PBS, and incubated for 30 min under agitation at 4 °C in RIPA buffer (10 mM Tris, 1 mM EDTA, 1% Triton X-100, 0.1% sodium deoxycholate, 0.1% SDS, 140 mM NaCl, 1 mM PMSF). Cell lysates were then centrifuged 20 min at 12,000 rpm at 4 °C and supernatants were collected. Protein concentrations were determined by Pierce BCA protein assay. Laemmli buffer (Biorad) and 2-mercaptoethanol (Sigma) (350 mM) were added to the protein samples. Finally, proteins were denatured by heating the samples at 100 °C for 5 min.

Nuclear fractions were obtained by scraping the cells and centrifuging the cells at 5000 rpm for 5 min. The cell pellet was then resuspended in cytoplasmic lysis buffer (10 mM HEPES, 0.1 mM EDTA, 10 mM KCl, NP40, 0.5 mM PMSF, 1 mM DTT, Protease inhibitor cocktail) and incubated on ice for 20 min with regular mixing, and then centrifuged at 12,000 rpm at 4 °C for 10 min. The supernatant was collected which consisted of the cytoplasmic extract. The nuclei pellet was washed with the cytoplasmic lysis buffer twice and resuspended in nuclear lysis buffer (20 mM HEPES, 125 mM NaCl, 1 mM EDTA, 1 mM PMSF, 1 mM DTT, Protease inhibitor cocktail). Lysates were sonicated for 5 s, placed on ice for 1 min and sonicated again for 5 s. Samples were incubated on ice for 30 min, centrifuged at 12,000×g for 15 min at 4 °C. The supernatant was collected which consisted of the nuclear extract. As above, protein concentrations were determined by Pierce BCA protein assay.

## Western blotting

The extracted proteins were separated on 10% SDS-PAGE gels and transferred to PVDF membrane (Thermofisher). Blots were incubated overnight with the primary antibody against PK-M2 (#21578, 1:1000, Signalway Antibody), Lamin A/C (#ab8984, 1:2000, Abcam), and GAPDH

(#AM4300, 1:5000, Ambion). The membranes were then incubated with secondary antibodies conjugated to horseradish peroxidase (HRP) (Santa Cruz Biotechnology) for 1 h at room temperature. The protein band detection was performed with ECL (solution A: 2.5 mM luminol, 0.4 mM p-coumaric acid, 0.1 M Tris-HCl; solution B: 0.02% hydrogen peroxide, 0.1 M Tris-HCl).

### PK-M2 flow cytometry

For PK-M2 flow cytometry study, cells were first fixed for 15 min at room temperature with 4% paraformaldehyde. Cells were then permeabilized with ice-cold methanol, for 10 min on ice. After several washes with PBS, fixed cells were incubated with primary antibody against PK-M2 (#21578, 1:100, Signalway Antibody) for 1 h at room temperature. Cells were washed before incubation with secondary antibody (Goat Anti-Rabbit IgG H&L, Alexa Fluor® 647, #ab150083, 1:500, Abcam) for 30 min at room temperature. Analysis was performed through flow cytometry.

### PK-M2 immunofluorescence

For PK-M2 immunofluorescence, 25,000 cells were seeded in Lab-Tek chamber slides (Thermofisher). Chambers were washed with PBS, and cells were incubated with 4% paraformaldehyde at 37 °C for 10 min and chilled on ice for 1 min. Cells were permeabilized by adding 90% methanol for 30 min on ice. Blocking was performed with 10% goat serum, for 30 min at room temperature under agitation. PK-M2 (#21578, rabbit, 1:100, Signalway Antibody) and Vimentin (#ab8069, mouse, 1:100, Abcam) primary antibodies were incubated for 30 min at room temperature, under agitation. Secondary antibodies (anti-rabbit IgG-TRITC, #T5268, 1:32, Sigma; anti-mouse IgG (H + L) Alexa Fluor 488, #62-6511, 1:100, Invitrogen) were added and incubated in the dark at room temperature for 30 min. Lastly, cells were counterstained with DAPI. Images were taken with Keyence BZ-9000 microscope (Keyence Corporation of America, Itasca, IL).

### RNA extraction and RT-qPCR

RNA was isolated from cells with TRIzol reagent (Ambion) according to the manufacturer's recommendations. RNA levels were measured with Nanodrop spectrophotometer (Thermofisher). Complementary DNA synthesis was performed on 1 µg of isolated RNA by using cDNA synthesis kit (Genesee Scientific). Quantitative PCR was done with qPCR-BIO SyGreen Mix lo-ROX (Genesee Scientific) according to manufacturer's instructions. Primers were purchased from Thermofisher. PK-M2: Fw. 5′-ATTATTTGAGGAACT CCGCCGCCT-3′; Rev, 5′- ATTCCGGGTCACAGCAAT GATGG-3′, RPLP0: Fw, 5′- GTGATGTGCAGCTGATCA AGACT-3′, Rev, 5′- GATGACCAGCCCAAAGGAGA-3′).

### Pyruvate kinase assay

Single cell suspensions of SUM159PT monolayers were seeded on 24-well tissue culture-treated plates, in duplicates. The cells were allowed to attach overnight and the next day cells were treated with either 1 mM $H_2O_2$, 10 µM TEPP46, or a single dose of 8 Gy. Cells were removed from one set of the wells from each treatment group and the number of live cells was determined by staining with trypan blue and counting with a hemocytometer. The other set of wells was used for determination of pyruvate kinase activity in each group via the Pyruvate Kinase Assay kit (Abcam, #ab83432) according to the manufacturer's instructions. Briefly, cells were washed once with PBS, followed by addition of pyruvate kinase assay buffer to each well for cell lysis. The cell lysate mixture was diluted to contain 2000 cells/50 µL (based on the cell numbers obtained with the trypan blue counting) with assay buffer and 50 µL of the cell lysate from each group was transferred to 96-well plates. Then, 50 µL of the master reaction mix was added to each sample. The optical density ($OD_{570nm}$) was measured as a function of time using a plate reader (SpectraMax M5, Molecular Devices, Sunnyvale, CA) at room temperature every minute for a total of 15 min. The signal increase per unit of time correlates with the amount of pyruvate generated by pyruvate kinase. Two $OD_{570nm}$ values ($A_1$ and $A_2$) within the linear range of the reaction for each sample were identified. The $\Delta A = A_2 - A_1$ was determined and plotted for each group. Three biologically independent experiments were performed for each experimental group.

## Results

### Exposure to radiation induces metabolic changes in TNBC cells

To determine overall metabolic changes in TNBC cells induced by radiation, we first evaluated radiation-induced changes in glucose uptake and lactate production over 3 days in SUM159PT and MDA-MB-231 TNBC cells. Glucose uptake was measured via flow cytometry using the fluorescent analogue of glucose 2NBDG or radiolabeled glucose ($^{18}$FDG). Both cell lines showed significantly more glucose uptake in the irradiated (8 Gy) compared to the non-irradiated controls by 24 h (Fig. 1a), and this continued for up to 3 days, which is the latest time point measured (Fig. 1a and Supplementary Fig. 1A). These data suggest that surviving cells significantly re-wire glucose metabolism for an extended period of time, relative to the non-irradiated cells.

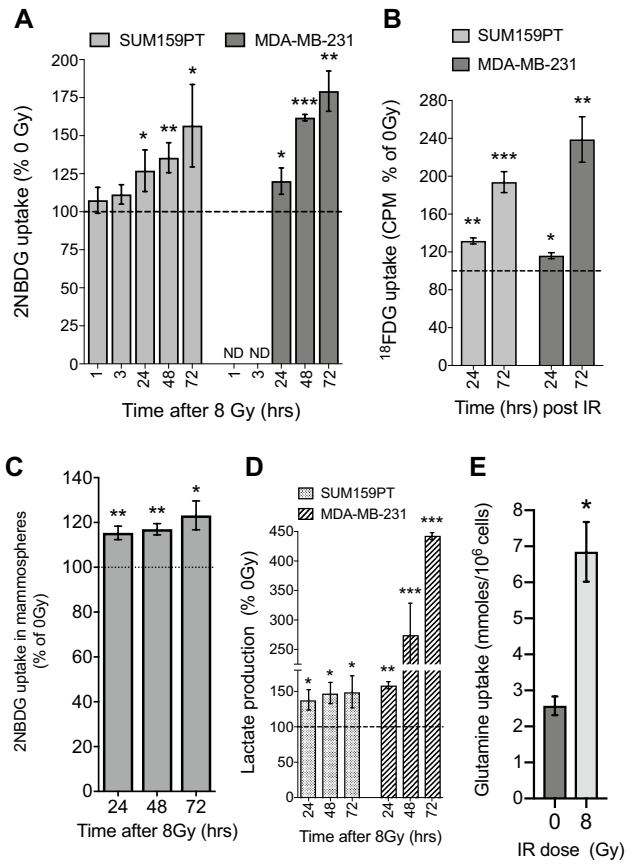


**Fig. 1** Exposure to IR modifies breast cancer cells metabolism. SUM159PT and MDA-MB-231 cells were seeded as monolayers and irradiated with a single dose of 8 Gy. At the indicated time points after irradiation cells were incubated with a fluorescent glucose analogue (2NBDG, **a**) or a radiolabeled glucose analogue ($^{18}$FDG, **b**) and glucose uptake was determined. **c** SUM159PT cells were grown as mammospheres and irradiated with a single dose of 8 Gy. At different time points after irradiation, cells were dissociated and incubated with 2NBDG and glucose uptake was determined via flow cytometry. **d** Lactate levels were measured in the media of irradiated SUM159PT and MDA-MB-231 monolayers at 24, 48 and 72 h after irradiation and normalized to the non-irradiated cells. **e** SUM159PT monolayer cells were irradiated with 8 Gy and 24 h later the media was collected and the concentration of glutamine in the media was determined via a Glutamine detection assay kit. **a–d** All results shown are normalized to 0 Gy controls (100%, dotted line). Paired, 2-tailed *t* test: $*P<0.05$, $**P<0.01$, $***P<0.001$

Interestingly, the increase in glucose uptake 24 h following irradiation was partially prevented when cells were irradiated in the presence of a potent anti-oxidant, the reduced form of glutathione (GSH), which scavenges IR-induced reactive oxygen species (ROS) (Supplementary Fig. 1B, C). This suggested that the metabolic reprogramming induced by radiation could be due, at least in part, to the ROS generated by radiation.

The IR-induced increase in glucose uptake in both TNBC lines was further confirmed using radiolabeled glucose ($^{18}$FDG) (Fig. 1b). Due to cell death caused by IR, irradiated cell cultures are less dense than the unirradiated ones at all the time points. Therefore, in order to exclude culture density as an artifact, we determined glucose uptake in non-irradiated cell cultures as a function of time and cell density. As shown in Supplementary Fig. 2A–C, glucose uptake increases, rather than decreases with higher cell density. In addition, cell lines are often propagated in culture media containing supraphysiological levels of glucose, which could confound glucose uptake measurements. Therefore, we also tested the effect of IR on glucose uptake in cells propagated in media containing physiological levels of glucose (~5.6 mM). Interestingly, glucose uptake at basal levels increased when cells were propagated under physiological levels of glucose; however, similar radiation-induced increases in glucose uptake were observed (Supplementary Fig. 2D). Finally, TNBC cells propagated as mammospheres in serum-free media enriched for breast cancer stem cells (BCSCs) [34] also increased glucose uptake after irradiation (Fig. 1c). These results suggested that the increase in glucose uptake by TNBC cells is a general phenomenon in different sub-types of breast cancer cells.

We next determined the effect of radiation on lactate production and observed that the increase in glucose uptake after radiation was accompanied by an increase in lactate production (Fig. 1d). Although 48 h after radiation no further increase was observed in SUM159PT cells, lactate production was still accumulating at 48 and 72 h in MDA-MB-231 cells, with a four-fold increase 72 h post irradiation (Fig. 1d). Since some of the lactate can also be derived from glutamine [35], we also measured glutamine consumption in irradiated cells. Indeed, irradiated cells consumed significantly more glutamine than non-irradiated controls 24 h after irradiation (Fig. 1e). Together, these results led us to conclude that TNBC cells that survive radiation robustly reprogram their metabolism independently of the cell culture system, and that this metabolic response must be important for cell survival and radioresistance.

## Radiation affects expression, localization and enzyme activity of PK-M2

The increase in glucose uptake, accompanied by an increase in lactate production (Fig. 1) suggested an enhanced glycolytic phenotype (Warburg effect [19, 36]) in irradiated TNBC cells. One of the main glycolytic enzymes that is often re-expressed in cancer cells and regulates flux through glycolysis is the M2 isoform of pyruvate kinase (PK-M2) [15, 22]. PK-M2 catalyzes the conversion of phosphoenol pyruvate (PEP) to pyruvate, which, in turn is converted to lactate. Therefore, we decided to determine the effect of radiation on the gene and protein expression levels of PK-M2. Interestingly, PK-M2 mRNA and protein expression levels

were significantly upregulated post irradiation (Fig. 2a, b and Supplementary Fig. 3A–C).

We next determined the effect of IR on the pyruvate kinase enzymatic activity of PK-M2. Although IR modestly increased PK-M2 enzymatic activity at 15 min and 3 h after irradiation (Fig. 2c), the PK activity was significantly inhibited 24 h after irradiation (Fig. 2c). As expected, and in agreement with a previous report [14] $H_2O_2$ significantly inhibited PK-M2 activity within 15 min of exposure (Supplementary Fig. 3D). In contrast, a small molecule *activator* of PK-M2 (TEPP46) [28, 37] significantly increased PK-M2 enzymatic activity only 1 h after treatment (Supplementary Fig. 3D). Importantly, preventing the inhibition of PK-M2 enzymatic activity by radiation via the small molecule activator TEPP46, partly reversed the IR-induced increase in lactate production by the irradiated cells (Fig. 2d). These findings suggested that the radiation-induced changes in PK-M2 levels and enzyme activity are regulating, at least in part, the metabolic changes occurring in irradiated TNBC cells. Interestingly however, although PK-M2 activation (via TEPP46) had a tendency to increase glucose uptake levels in non-irradiated and irradiated cells, it did not significantly alter them (Supplementary Fig. 3E).

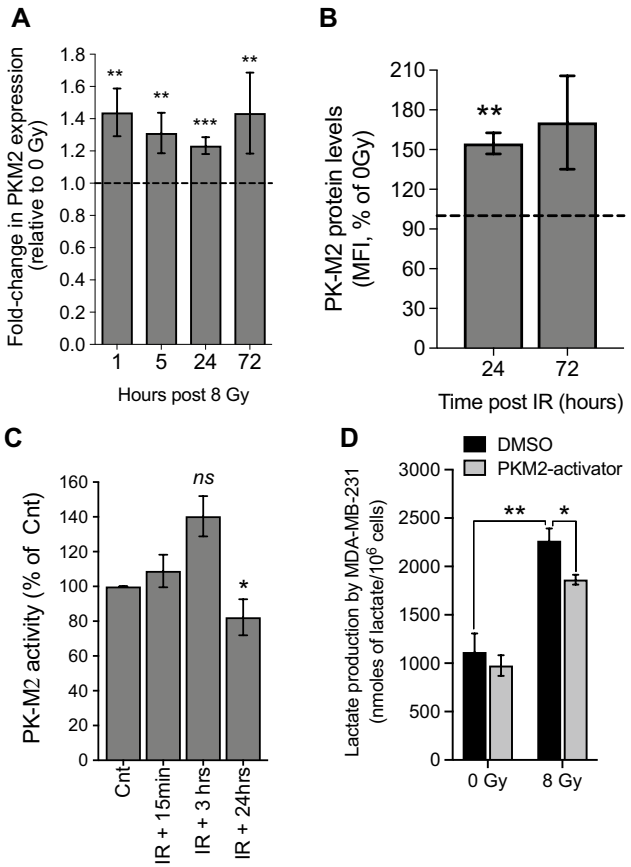


**Fig. 2** Radiation modulates PK-M2 expression levels and its enzymatic activity. **a** PK-M2 gene expression levels were determined in SUM159PT monolayers at 1, 5, 24, and 72 h after a single dose of 8 Gy. Results shown are normalized to 0 Gy control (dotted line). Paired, 2-tailed *t* test: $^{**}P<0.01$, $^{***}P<0.001$. **b** SUM159PT monolayers were irradiated with 0 or 8 Gy. Cells were fixed, permeabilized and immunostained for the PK-M2 protein. PK-M2 protein expression levels were determined by flow cytometry at 24 and 72 h after irradiation. PK-M2 mean fluorescence intensity was measured and normalized to 0 Gy controls (100%, dotted line). Paired, 2-tailed *t* test: $^{**}P<0.01$. **c** SUM159PT cells were irradiated with a single dose of 8 Gy. Pyruvate kinase activity was then measured at the indicated time points. Results shown are normalized to 0 Gy non-treated control (Cnt). Paired, 2-tailed *t* test: $^{*}P<0.05$. **d** MDA-MB-231 cells were treated with 10 µM TEPP46 3 h prior to irradiation followed by another treatment 24 h later. Media was collected 3 h after the second TEPP46 treatment and lactate levels were measured. Paired, 2-tailed *t* test: $^{*}P<0.05$, $^{**}P<0.01$

Unlike PK-M1, which is a constitutively active tetramer, PK-M2 has conformational flexibility and can readily switch between enzymatically-inactive dimers and active tetramers. Therefore, one interpretation of the observation that, in irradiated cells, PK-M2 enzymatic activity is reduced despite the increase in its expression and protein levels, is that after irradiation most of the PK-M2 protein exists in the enzymatically-inactive dimeric form. PK-M2 dimers are often found in the nucleus and have been implicated in gene regulation [23, 25, 38]. We therefore investigated whether IR affected the cellular localization of PK-M2 using immunofluorescence and western blotting of nuclear fractions. As expected, immunofluorescence studies showed that while non-irradiated cells showed weak nuclear staining for PK-M2, upon irradiation the fraction of cells with nuclear PK-M2 was increased (Fig. 3a, b). This observation was confirmed by western blotting of nuclear fractions of irradiated and non-irradiated SUM159PT cells (Supplementary Fig. 4A). Interestingly, irradiating TNBC cells in the presence of GSH partially prevented the nuclear translocation of PK-M2 (Fig. 3c) suggesting that the ROS generated by radiation is contributing to the nuclear translocation of PK-M2. In addition, although cancer cells in general exhibit high glucose uptake (Warburg effect [19, 36]), heterogeneity exists (Supplementary Fig. 4B). In light of our findings that radiation induces an increase in glucose uptake (Fig. 1a–c) it seems that high glucose consumption may be an important factor in surviving oxidative stress, such as induced by radiation. Therefore, we decided to determine the relationship between glucose uptake levels and nuclear PK-M2. For this, SUM159PT cells were labeled with 2NBDG and sorted into populations with low ($2NBDG^{low}$) or high ($2NBDG^{high}$) glucose uptake (Supplementary Fig. 4B). The cells were plated on microscope chamber slides and the next day immunostained for PK-M2 (Supplementary Fig. 4C). Interestingly, a higher fraction of $2NBDG^{low}$ cells contained nuclear PK-M2 compared to $2NBDG^{high}$ (Fig. 3d and Supplementary Fig. 4C).

The above data strongly suggested that the enzymatically-inactive, dimeric form of PK-M2 is mediating metabolic changes that might be important for cancer cell

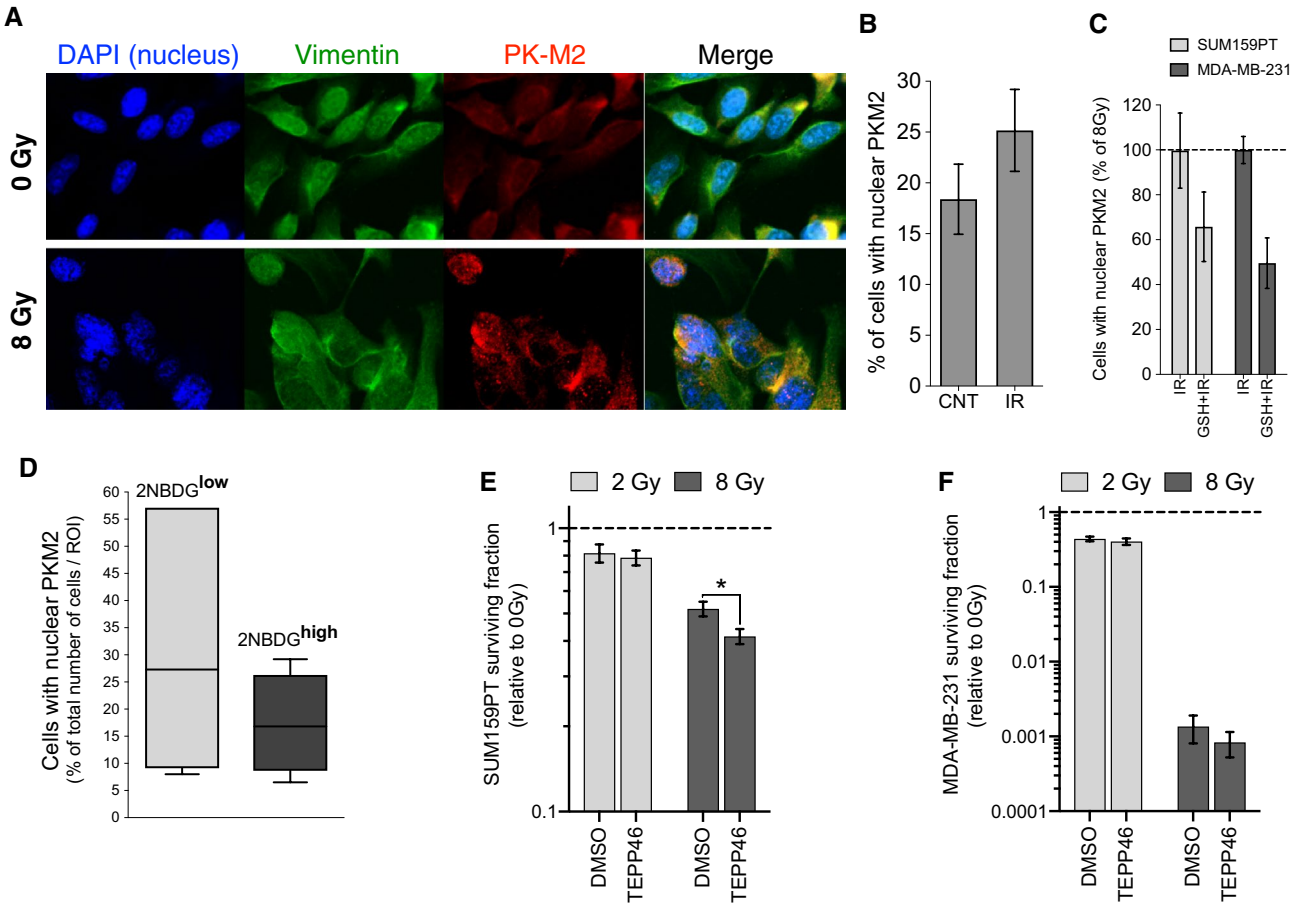


**Fig. 3** Radiation induces nuclear translocation of PK-M2 and PK-M2 activators enhance the effect of radiation on differentiated BC cells. **a** SUM159PT cells were seeded as monolayers in microscope chamber slides and irradiated with a single dose of 8 Gy. PK-M2 (red) and vimentin (green) were immunostained and nuclei were counterstained with DAPI (blue). Cells were visualized via confocal microscopy (60X). **b** SUM159PT cells were immunostained as in A, and cells were visualized via fluorescence microscopy. The fraction of cells with nuclear PK-M2 was determined by counting the number of cells with PK-M2 staining in the nucleus and dividing by the total number of cells in the field of view (FOV). > 30 FOVs were used to determine the average fraction. **c** SUM159PT and MDA-MB-231 cells were seeded and irradiated with a single dose of 8 Gy, with or without GSH (2.5 mM) ($n = 3$–4). As in A, cells were immunostained for PK-M2 and cells with nuclear PK-M2 were counted and normalized to the 8 Gy group (dotted line). **d** Sorted 2NBDG-low and 2NBDG-high cells were seeded on microscope chamber slides and allowed to adhere overnight. The next day cells were fixed, permeabilized and immunostained for the PK-M2 protein and the nuclei were counterstained with DAPI. The fraction of cells with nuclear PK-M2 was determined by counting the number of cells with PK-M2 staining in the nucleus and dividing by the total number of cells in the field of view (FOV). > 30 FOVs were used to determine the average fraction. **e, f** SUM159PT and MDA-MB-231 cells were treated with DMSO or TEPP46 (10 µM) as monolayers. Cells were then detached, irradiated with 2 or 8 Gy, and plated at clonogenic density in 6-well plates. After 10 to 15 days, cells were fixed and stained, and colonies were then counted. The results were normalized to 0 Gy controls. Paired, 2-tailed *t* test: $^*P < 0.05$

survival under oxidative stress, such as during radiation therapy. Therefore, we reasoned that PK-M2 activators might sensitize TNBC cells to irradiation. To test this, we irradiated TNBC cells derived from either unselected cultures propagated as adherent monolayers in serum-supplemented conditions or as BCSC-enriched mammosphere cultures in serum-free conditions, and performed either classical colony formation assays or extreme limiting dilution (mammosphere) assays (ELDA) [39]. Activating PK-M2 (via TEPP46) in adherent cultures had no effect on their plating efficiency (Supplementary Fig. 4D) or the surviving fraction at 2 Gy for both TNBC lines (Fig. 3e, f, light gray bars). However, PK-M2 activation did sensitize adherent cells to 8 Gy (Fig. 3e, f, dark gray bars). Importantly, the sensitizing effect of activating PK-M2 was greatly enhanced in the BCSC-enriched cell populations as demonstrated by the cancer stem cell frequencies determined by ELDA [40] (Fig. 4a, b). It is worth noting here that PK-M2 activation also significantly reduced intrinsic BCSC frequencies for both TNBC lines (Fig. 4a, b, SUM159PT, DMSO vs. TEPP, $p = 0.00316$; MDA-MB-231, DMSO vs. TEPP, $p = 0.0103$).

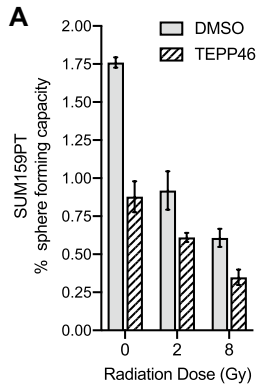


| SUM159PT | 1/CSC frequency | 95% CI | Pairwise tests for differences in stem cell frequencies (*p* value) | |
|---|---|---|---|---|
| DMSO | **13.7** | 19.9-9.4 | DMSO *vs.* 2Gy | ***0.000181*** |
| 2Gy | **37.9** | 54.9-26.2 | DMSO *vs.* 8Gy | ***1.24E-07*** |
| 8Gy | **59** | 85.6-40.7 | DMSO *vs.* TEPP | ***0.00316*** |
| TEPP | **31.2** | 45.3-21.6 | 2Gy *vs.* 2Gy + TEPP | *0.415* |
| 2Gy + TEPP | **47.4** | 68.9-32.7 | 8Gy *vs.* 8Gy + TEPP | ***0.00118*** |
| 8Gy + TEPP | **144** | 208.3-99.5 | TEPP *vs.* 2Gy + TEPP | *0.139* |
| | | | TEPP *vs.* 8Gy + TEPP | ***3.96E-08*** |

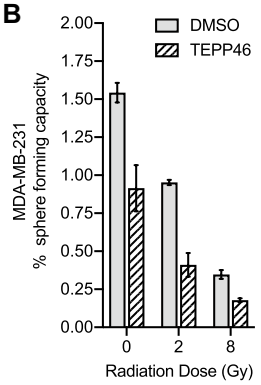


| MDA-MB-231 | 1/CSC frequency | 95% CI | Pairwise tests for differences in stem cell frequencies (*p* value) | |
|---|---|---|---|---|
| DMSO | **30.6** | 44.6-21 | DMSO *vs.* 2Gy | *0,291* |
| 2Gy | **41.1** | 59.7-28.3 | DMSO *vs.* 8Gy | ***5,48E-05*** |
| 8Gy | **94.7** | 137.6-65.2 | DMSO *vs.* TEPP | ***0,0103*** |
| TEPP | **61.9** | 89.8-42.7 | 2Gy *vs.* 2Gy + TEPP | ***0,0011*** |
| 2Gy + TEPP | **102.1** | 147.9-70.5 | 8Gy *vs.* 8Gy + TEPP | ***0,00144*** |
| 8Gy + TEPP | **229.2** | 331.8-158.3 | TEPP *vs.* 2Gy + TEPP | *0,0695* |
| | | | TEPP *vs.* 8Gy + TEPP | ***1,54E-06*** |

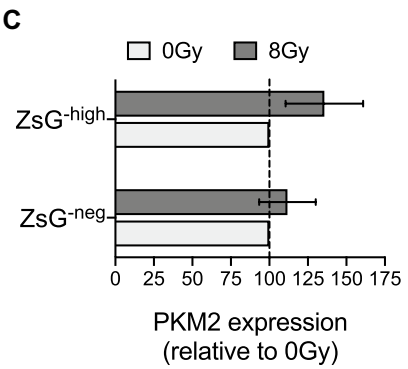


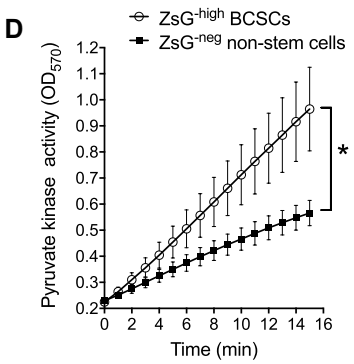


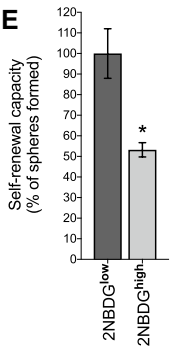


**Fig. 4** PK-M2 activators enhance the effect of radiation on the radioresistant BCSC population. **a**, **b** SUM159PT and MDA-MB-231 were seeded into low adhesion 96-well plates, irradiated with a single dose of 2 Gy or 8 Gy, and treated every day for 5 days with TEPP46 (10 μM). The number of spheres formed was counted 7 days after seeding. Left panels show the percentage of sphere forming capacity defined by the number of spheres formed relative to the number of cells plated. Right panels show the analysis through ELDA (Extreme Limiting Dilution Analysis) software and represent the CSC frequency as 1/CSC frequency. **c** SUM159PT-ZsGreen cells were plated and irradiated with a single dose of 8 Gy. Cells were fixed and immunostained for PKM2 expression 24 h later, and then analyzed by flow cytometry. Geometric mean fluorescence were normalized to 0 Gy controls. **d** SUM159PT-ZsGreen cells were sorted and PKM2 kinase activity was assessed in the $ZsG^{-high}$ population as well as in $ZsG^{-neg}$ cells. Paired, 2-tailed *t* test: $^{*}P < 0.05$. **e** Sorted 2NBDG-low and 2NBDG-high SUM159PT cells were seeded in mammosphere-forming conditions in serum-free media on 96-well plates. Cells were allowed to form mammospheres for ~ 10 days and the % of cells capable of forming mammospheres was determined by counting the number of spheres per well

## PK-M2 and breast cancer stem cells

The remarkable effect of PK-M2 activation on the frequency of BCSCs either at basal levels or after irradiation (Fig. 4a, b) led us to further investigate the status of PK-M2 in BCSCs. For these experiments we used a fluorescent reporter (ZsGreen-cODC) for BCSCs that is based on low proteasome activity of CSCs, a characteristic of BCSCs that we, and others have previously reported [32, 33, 41–51]. Differentiated cells have high proteasome activity that leads to immediate degradation of the fluorescent protein reporter (ZsGreen-negative), while BCSCs with low proteasome

activity accumulate the fluorescent protein (ZsGreen-positive) and can thus readily be identified and isolated based on cell-associated fluorescence. SUM159PT cells stably expressing the reporter (SUM159PT-ZsGreen) were irradiated and 24 h later immunostained for PK-M2. The PK-M2 protein levels in the non-stem, ZsGreen-neg cells and ZsGreen-pos BCSCs were assessed via flow cytometry. Interestingly, the protein levels of PK-M2 were similar in the two cell populations at basal level (Supplementary Fig. 4E) and both the ZsGreen-neg and the ZsGreen-pos populations increased PKM2 levels after irradiation (Fig. 4c), similar to the unselected population of cells (Fig. 2b). However, the increase in PKM2 levels was greater in the BCSC population (Fig. 4c), suggesting an enhanced role for PKM2 in the BCSC that could explain in part the sensitivity to PK-M2 activators (Fig. 4a, b). To further explore this possibility we also compared the pyruvate kinase activity of the ZsGreen-neg non-stem cell population with the ZsGreen-pos BCSCs. Surprisingly, the PK activity of BCSCs was significantly higher compared to that of non-stem cells (Fig. 4d). These results suggested that the relative abundance of PK-M2 tetramers with respect to dimers is greater in the BCSC population compared to the non-stem (ZsGreen-neg) cells. Interestingly, and in agreement with a quiescent phenotype of BCSCs, cells with low glucose uptake ($2NBDG^{low}$) formed significantly more mammospheres compared to the population of cells with high glucose uptake ($2NBDG^{high}$) (Fig. 4e). Together with the observation that $2NBDG^{low}$ cells are also enriched for cells with nuclear PK-M2, these data suggest that nuclear PK-M2 may maintain a stemness phenotype in BCSCs that have low, basal glucose uptake levels and are less glycolytically active.

## Discussion

Studies with normal cells show that metabolic reprogramming is required for cells to survive lethal oxidative stress [12, 52]. Normal cells exposed to chemically-induced oxidative stress can immediately (seconds to minutes) shuttle glucose into the pentose phosphate pathway (PPP) [12, 29, 52]. Such acute metabolic reprogramming, which precedes transcriptional responses, generates reducing equivalents in the form of nicotinamide adenine dinucleotide phosphate (NADPH) that help neutralize potentially lethal levels of ROS and maintain cellular redox balance [29]. The study put forth here demonstrates that TNBC cells exposed to oxidative stress through IR reprogram their metabolism by increasing the long-term utilization of glucose, consuming more glutamine and producing more lactate (Fig. 1). Oxidative stress induced by chemical means ($H_2O_2$) has been shown to rapidly re-wire metabolic flux in human lung cancer cells ultimately facilitating an anti-oxidant response which has been ascribed to the inhibition of the redox-sensitive pyruvate kinase activity of PK-M2 within 15 min of exposure as a result of the oxidation of a cysteine residue ($Cys^{358}$) [14]. In contrast, our results show that inhibition of PK-M2 activity via oxidative stress induced by radiation only became apparent and significant 24 h after radiation (Fig. 2c), suggesting that at least the initial radiation-induced ROS are insufficient to inactivate the enzyme. This observation is important in that it demonstrates that oxidative stress induced by chemical means, as a model for oxidative stress does not necessarily reflect the cellular response during radiation therapy used to treat most cancers.

The appreciable inhibition of the pyruvate kinase activity of PK-M2 by irradiation (Fig. 2c) seems contradictory with the observation that irradiated cells increase lactate production at the same time point (24 h post irradiation) (Fig. 1d). Theoretically, reduced activity of PK-M2 after radiation should result in less pyruvate production, which should in turn result in less pyruvate available for lactate formation. However, other groups have shown that the conversion of pyruvate to either lactate or acetyl-CoA, which then undergoes further oxidation by the mitochondria, is determined by the relative enzymatic activity of PKM2. Low enzymatic activity of PK-M2 promotes the conversion of pyruvate to lactate giving rise to the 'Warburg effect' observed in most cancers [19, 53], whereas high activity of PK-M2, similar to the constitutively active PK-M1, promotes conversion of pyruvate to acetyl-CoA [20–22, 54]. Therefore, our results suggest that the inhibition of PK-M2 enzymatic activity by radiation contributes to the increased levels of lactate production in irradiated TNBC cells. This conclusion is reenforced by the observation that preventing the radiation-induced inhibition of the enzymatic activity of PK-M2 via the small molecule activator, TEPP46 partially reverses the increase in lactate production after radiation (Fig. 2d). However, this does not exclude other possibilities for lactate production, such as the conversion of glutamine to lactate via glutaminolysis that could further add to the pool of lactate produced by irradiated cells. Indeed, this possibility is supported by the increased levels of glutamine consumption in irradiated TNBC cells (Fig. 1e). Another contributing factor could be the changes in endogenous metabolite levels upstream of PK-M2 that are known allosteric activators of PK-M2 enzymatic activity, such as fructose-1,6-bisphosphate (FBP) or serine [55, 56]. Although we did not determine whether radiation induces changes in the levels of FBP or serine, others have shown that under (chemically-induced) oxidative stress glucose carbons are diverted away from glycolysis and shunted through the PPP [14] suggesting a decreased availability of glucose carbons for the generation of FBP or serine. This scenario would further promote an overall inactivation of the cellular PK-M2 pool, and as

a result contribute to the increased lactate production after irradiation.

Intriguingly, the radiation-induced decrease in pyruvate kinase activity of PK-M2 was accompanied by increases in mRNA and protein expression levels, suggesting that most of the PK-M2 protein existed in the enzymatically-inactive conformation (either monomers or dimers) after radiation. A number of studies have shown that PK-M2 dimers lack pyruvate kinase activity and translocate to the nucleus to regulate gene transcription [18, 23–26, 57, 58]. Some studies suggest that PK-M2 regulates transcription by acting as a protein kinase [23, 38, 59, 60], although the protein kinase activity of nuclear PK-M2 remains controversial [61]. In our study in TNBC cells, radiation-induced translocation of PK-M2 to the nucleus and this appeared to be ROS dependent (Fig. 3a–c). This finding agrees with a recent study showing that IR induces nuclear translocation of PK-M2 in glioblastoma multiforme cells and that nuclear PK-M2 participates in DNA repair after radiation by facilitating homologous recombination of DNA double strand breaks [62]. Interestingly, in our study, TNBC cells with low basal glucose uptake ($2NBDG^{low}$) were enriched for breast CSCs (Fig. 4e) and had a higher proportion of cells with nuclear PK-M2 (Fig. 3d) compared to those with high basal glucose uptake, suggesting that PK-M2 may play a role in maintaining "stemness" in TNBC cells. These results are consistent with the findings that PK-M2 plays a role in maintaining a "stem cell" phenotype in breast cancer cells via the Wnt/β-catenin pathway [18].

We had anticipated that the PK activity of BCSCs would be lower relative to the non-stem cell population as this would mean that BCSCs depend more on the enzymatically-inactive PK-M2 dimers and therefore would be more susceptible to PK-M2 activator that promote a tetrameric conformation, as shown in Fig. 4a, b. However, the surprising finding that BCSCs have significantly higher PK-M2 activity relative to the non-stem cell population agree with a quiescent phenotype for BCSCs and suggest that the depletion of BCSCs by PK-M2 activators is not mainly due to the effect on the pyruvate kinase activity, but that other factors are in play, such as the possibility of sequestering PK-M2 into the cytoplasm and out of the nucleus.

Finally, small molecule compounds that promote the tetrameric, enzymatically active conformation of PK-M2 have been developed and have been shown to prevent the nuclear translocation of PK-M2 [63], and have anti-proliferative effects on lung cancer cells [27, 37]. Importantly, our results show that these small molecule activators of PK-M2 can deplete breast CSCs in vitro (Fig. 4a, b), thus strongly suggesting that in addition to having anti-proliferative effects [27, 37] these activators could also impact the therapy-resistant stem cell compartment of tumors. These studies support the idea of combining PK-M2 activators with radiation to enhance the effect of radiation therapy in resistant cancers, such as TNBC.

**Acknowledgements** We would like to acknowledge Dr. William McBride for his careful editing of the manuscript and thoughtful feedback and comments.

**Author contributions** LZ and JB performed most of the experiments and data analysis and assisted with editing of the manuscript. TY, KD, DS, AD, LG, DN, KB, CA, and MBD assisted with experiments and data analysis. FP assisted with experimental design and editing of the manuscript. EV designed all experiments, oversaw data analysis, and wrote the manuscript.

**Funding** EV was supported by a Junior Faculty Award (JFA) from the American Society for Radiation Oncology (ASTRO) and the UCLA SPORE in Brain Cancer (P50 CA211015). FP was supported by grants from the National Cancer Institute (CA137110, CA161294).

## Compliance with ethical standards

**Conflict of interest** All authors declare that they have no conflicts of interest.

**Ethical approval** This article does not contain any studies with human participants or animals performed by any of the authors.

## References

1. Sjostrom M, Lundstedt D, Hartman L, Holmberg E, Killander F, Kovacs A, Malmstrom P, Nimeus E, Werner Ronnerman E, Ferno M et al (2017) Response to radiotherapy after breast-conserving surgery in different breast cancer subtypes in the swedish breast cancer group 91 radiotherapy randomized clinical trial. J Clin Oncol 35:3222–3229
2. Liedtke C, Mazouni C, Hess KR, Andre F, Tordai A, Mejia JA, Symmans WF, Gonzalez-Angulo AM, Hennessy B, Green M et al (2008) Response to neoadjuvant therapy and long-term survival in patients with triple-negative breast cancer. J Clin Oncol 26(8):1275–1281
3. Vlashi E, Pajonk F (2014) Cancer stem cells, cancer cell plasticity and radiation therapy. Semin Cancer Biol 31:28–35
4. Pajonk F, Vlashi E, McBride WH (2010) Radiation resistance of cancer stem cells: the 4 R's of radiobiology revisited. Stem cells (Dayton, Ohio) 28(4):639–648
5. Phillips TM, McBride WH, Pajonk F (2006) The response of CD24(-/low)/CD44 + breast cancer-initiating cells to radiation. J Natl Cancer Inst 98(24):1777–1785
6. Lagadec C, Vlashi E, Della Donna L, Dekmezian C, Pajonk F (2012) Radiation-induced reprogramming of breast cancer cells. Stem Cells (Dayton, Ohio) 30(5):833–844
7. Lagadec C, Vlashi E, Della Donna L, Meng Y, Dekmezian C, Kim K, Pajonk F (2010) Survival and self-renewing capacity of breast cancer initiating cells during fractionated radiation treatment. Breast Cancer Res 12(1):R13
8. Woodward WA, Chen MS, Behbod F, Alfaro MP, Buchholz TA, Rosen JM (2007) WNT/beta-catenin mediates radiation resistance of mouse mammary progenitor cells. Proc Natl Acad Sci USA 104(2):618–623
9. O'Neill P, Wardman P (2009) Radiation chemistry comes before radiation biology. Int J Radiat Biol 85(1):9–25

10. Liou GY, Storz P (2010) Reactive oxygen species in cancer. Free Radical Res 44(5):479–496
11. Colussi C, Albertini MC, Coppola S, Rovidati S, Galli F, Ghibelli L (2000) H2O2-induced block of glycolysis as an active ADP-ribosylation reaction protecting cells from apoptosis. FASEB J 14(14):2266–2276
12. Ralser M, Wamelink MM, Kowald A, Gerisch B, Heeren G, Struys EA, Klipp E, Jakobs C, Breitenbach M, Lehrach H et al (2007) Dynamic rerouting of the carbohydrate flux is key to counteracting oxidative stress. J Biol 6(4):10
13. Ralser M, Wamelink MM, Latkolik S, Jansen EE, Lehrach H, Jakobs C (2009) Metabolic reconfiguration precedes transcriptional regulation in the antioxidant response. Nat Biotechnol 27(7):604–605
14. Anastasiou D, Poulogiannis G, Asara JM, Boxer MB, Jiang JK, Shen M, Bellinger G, Sasaki AT, Locasale JW, Auld DS et al (2011) Inhibition of pyruvate kinase M2 by reactive oxygen species contributes to cellular antioxidant responses. Science (New York, NY) 334(6060):1278–1283
15. Eigenbrodt E, Reinacher M, Scheefers-Borchel U, Scheefers H, Friis R (1992) Double role for pyruvate kinase type M2 in the expansion of phosphometabolite pools found in tumor cells. Crit Rev Oncog 3(1–2):91–115
16. Chaneton B, Gottlieb E (2012) Rocking cell metabolism: revised functions of the key glycolytic regulator PKM2 in cancer. Trends Biochem Sci 37(8):309–316
17. Dayton TL, Jacks T, Vander Heiden MG (2016) PKM2, cancer metabolism, and the road ahead. EMBO Rep 17(12):1721–1730
18. Zhao Z, Song Z, Liao Z, Liu Z, Sun H, Lei B, Chen W, Dang C (2016) PKM2 promotes stemness of breast cancer cell by through Wnt/beta-catenin pathway. Tumour Biol 37(3):4223–4234
19. Warburg O (1924) On the metabolism of carcinoma cells. Biochem Z 152(309–344):309
20. Vander Heiden MG, Cantley LC, Thompson CB (2009) Understanding the Warburg effect: the metabolic requirements of cell proliferation. Science (New York, NY) 324(5930):1029–1033
21. Christofk HR, Vander Heiden MG, Wu N, Asara JM, Cantley LC (2008) Pyruvate kinase M2 is a phosphotyrosine-binding protein. Nature 452(7184):181–186
22. Christofk HR, Vander Heiden MG, Harris MH, Ramanathan A, Gerszten RE, Wei R, Fleming MD, Schreiber SL, Cantley LC (2008) The M2 splice isoform of pyruvate kinase is important for cancer metabolism and tumour growth. Nature 452(7184):230–233
23. Gao X, Wang H, Yang JJ, Liu X, Liu ZR (2012) Pyruvate kinase M2 regulates gene transcription by acting as a protein kinase. Mol Cell 45(5):598–609
24. Lee J, Kim HK, Han YM, Kim J (2008) Pyruvate kinase isozyme type M2 (PKM2) interacts and cooperates with Oct-4 in regulating transcription. Int J Biochem Cell Biol 40(5):1043–1054
25. Yang W, Lu Z (2013) Nuclear PKM2 regulates the Warburg effect. Cell Cycle (Georgetown, Tex) 12(19):3154–3158
26. Yang W, Xia Y, Ji H, Zheng Y, Liang J, Huang W, Gao X, Aldape K, Lu Z (2011) Nuclear PKM2 regulates beta-catenin transactivation upon EGFR activation. Nature 480(7375):118–122
27. Anastasiou D, Yu Y, Israelsen WJ, Jiang JK, Boxer MB, Hong BS, Tempel W, Dimov S, Shen M, Jha A et al (2012) Pyruvate kinase M2 activators promote tetramer formation and suppress tumorigenesis. Nat Chem Biol 8(10):839–847
28. Boxer MB, Jiang JK, Vander Heiden MG, Shen M, Skoumbourdis AP, Southall N, Veith H, Leister W, Austin CP, Park HW et al (2010) Evaluation of substituted N, N'-diarylsulfonamides as activators of the tumor cell specific M2 isoform of pyruvate kinase. J Med Chem 53(3):1048–1055
29. Kuehne A, Emmert H, Soehle J, Winnefeld M, Fischer F, Wenck H, Gallinat S, Terstegen L, Lucius R, Hildebrand J et al (2015) Acute activation of oxidative pentose phosphate pathway as first-line response to oxidative stress in human skin cells. Mol Cell 59(3):359–371
30. Le Goffe C, Vallette G, Charrier L, Candelon T, Bou-Hanna C, Bouhours JF, Laboisse CL (2002) Metabolic control of resistance of human epithelial cells to H2O2 and NO stresses. Biochem J 364(Pt 2):349–359
31. Vlashi E, Lagadec C, Vergnes L, Reue K, Frohnen P, Chan M, Alhiyari Y, Dratver MB, Pajonk F (2014) Metabolic differences in breast cancer stem cells and differentiated progeny. Breast Cancer Res Treat 146(3):525–534
32. Vlashi E, Lagadec C, Vergnes L, Matsutani T, Masui K, Poulou M, Popescu R, Della Donna L, Evers P, Dekmezian C et al (2011) Metabolic state of glioma stem cells and nontumorigenic cells. Proc Natl Acad Sci USA 108(38):16062–16067
33. Vlashi E, Kim K, Lagadec C, Donna LD, McDonald JT, Eghbali M, Sayre JW, Stefani E, McBride W, Pajonk F (2009) In vivo imaging, tracking, and targeting of cancer stem cells. J Natl Cancer Inst 101(5):350–359
34. Dontu G, Abdallah WM, Foley JM, Jackson KW, Clarke MF, Kawamura MJ, Wicha MS (2003) In vitro propagation and transcriptional profiling of human mammary stem/progenitor cells. Genes Dev 17(10):1253–1270
35. Jin L, Alesi GN, Kang S (2016) Glutaminolysis as a target for cancer therapy. Oncogene 35(28):3619–3625
36. Warburg O, Wind F, Negelein E (1927) The metabolism of tumors in the body. J Gen Physiol 8(6):519–530
37. Walsh MJ, Brimacombe KR, Anastasiou D, Yu Y, Israelsen WJ, Hong BS, Tempel W, Dimov S, Veith H, Yang H et al (2010) ML265: a potent PKM2 activator induces tetramerization and reduces tumor formation and size in a mouse xenograft model. In: Probe Reports from the NIH Molecular Libraries Program. Bethesda
38. Lv L, Xu YP, Zhao D, Li FL, Wang W, Sasaki N, Jiang Y, Zhou X, Li TT, Guan KL et al (2013) Mitogenic and oncogenic stimulation of K433 acetylation promotes PKM2 protein kinase activity and nuclear localization. Mol Cell 52(3):340–352
39. Hu Y, Smyth GK (2009) ELDA: extreme limiting dilution analysis for comparing depleted and enriched populations in stem cell and other assays. J Immunol Methods 347(1–2):70–78
40. http://www.bioinfwehieduau/software/elda/
41. Adikrisna R, Tanaka S, Muramatsu S, Aihara A, Ban D, Ochiai T, Irie T, Kudo A, Nakamura N, Yamaoka S et al (2012) Identification of pancreatic cancer stem cells and selective toxicity of chemotherapeutic agents. Gastroenterology 143(1):234–245
42. Della Donna L, Lagadec C, Pajonk F (2012) Radioresistance of prostate cancer cells with low proteasome activity. Prostate 72(8):868–874
43. Hayashi K, Tamari K, Ishii H, Konno M, Nishida N, Kawamoto K, Koseki J, Fukusumi T, Kano Y, Nishikawa S et al (2014) Visualization and characterization of cancer stem-like cells in cervical cancer. Int J Oncol 45:2468–2474
44. Lagadec C, Vlashi E, Bhuta S, Lai C, Mischel P, Werner M, Henke M, Pajonk F (2014) Tumor cells with low proteasome subunit expression predict overall survival in head and neck cancer patients. BMC Cancer 14:152
45. Munakata K, Uemura M, Tanaka S, Kawai K, Kitahara T, Miyo M, Kano Y, Nishikawa S, Fukusumi T, Takahashi Y et al (2016) Cancer stem-like properties in colorectal cancer cells with low proteasome activity. Clinical Cancer Res 22(21):5277–5286
46. Muramatsu S, Tanaka S, Mogushi K, Adikrisna R, Aihara A, Ban D, Ochiai T, Irie T, Kudo A, Nakamura N et al (2013) Visualization of stem cell features in human hepatocellular carcinoma reveals in vivo significance of tumor-host interaction and clinical course. Hepatology 58(1):218–228

47. Pan J, Zhang Q, Wang Y, You M (2010) 26S proteasome activity is down-regulated in lung cancer stem-like cells propagated in vitro. PLoS ONE 5(10):e13298
48. Stacer AC, Wang H, Fenner J, Dosch JS, Salomonnson A, Luker KE, Luker GD, Rehemtulla A, Ross BD (2015) Imaging reporters for proteasome activity identify tumor- and metastasis-initiating cells. Mol Imaging 14:414–428
49. Tamari K, Hayashi K, Ishii H, Kano Y, Konno M, Kawamoto K, Nishida N, Koseki J, Fukusumi T, Hasegawa S et al (2014) Identification of chemoradiation-resistant osteosarcoma stem cells using an imaging system for proteasome activity. Int J Oncol 45:2349–2354
50. Tang B, Raviv A, Esposito D, Flanders KC, Daniel C, Nghiem BT, Garfield S, Lim L, Mannan P, Robles AI et al (2015) A flexible reporter system for direct observation and isolation of cancer stem cells. Stem cell Rep 4(1):155–169
51. Vlashi E, Lagadec C, Chan M, Frohnen P, McDonald AJ, Pajonk F (2013) Targeted elimination of breast cancer cells with low proteasome activity is sufficient for tumor regression. Breast Cancer Res Treat 141(2):197–203
52. Grant CM (2008) Metabolic reconfiguration is a regulated response to oxidative stress. J Biol 7(1):1
53. Warburg O (1925) On the formation of lactic acid with growth. Biochem Z 160:307–311
54. Tamada M, Suematsu M, Saya H (2012) Pyruvate kinase M2: multiple faces for conferring benefits on cancer cells. Clin Cancer Res 18(20):5554–5561
55. Jurica MS, Mesecar A, Heath PJ, Shi W, Nowak T, Stoddard BL (1998) The allosteric regulation of pyruvate kinase by fructose-1,6-bisphosphate. Structure 6(2):195–210
56. Chaneton B, Hillmann P, Zheng L, Martin ACL, Maddocks ODK, Chokkathukalam A, Coyle JE, Jankevics A, Holding FP, Vousden KH et al (2012) Serine is a natural ligand and allosteric activator of pyruvate kinase M2. Nature 491(7424):458–462
57. Luo W, Hu H, Chang R, Zhong J, Knabel M, O'Meally R, Cole RN, Pandey A, Semenza GL (2011) Pyruvate kinase M2 is a PHD3-stimulated coactivator for hypoxia-inducible factor 1. Cell 145(5):732–744
58. Wang HJ, Hsieh YJ, Cheng WC, Lin CP, Lin YS, Yang SF, Chen CC, Izumiya Y, Yu JS, Kung HJ et al (2014) JMJD5 regulates PKM2 nuclear translocation and reprograms HIF-1alpha-mediated glucose metabolism. Proc Natl Acad Sci USA 111(1):279–284
59. Yu X, Li S (2017) Non-metabolic functions of glycolytic enzymes in tumorigenesis. Oncogene 36(19):2629–2636
60. Cheng TY, Yang YC, Wang HP, Tien YW, Shun CT, Huang HY, Hsiao M, Hua KT (2018) Pyruvate kinase M2 promotes pancreatic ductal adenocarcinoma invasion and metastasis through phosphorylation and stabilization of PAK2 protein. Oncogene
61. Hosios AM, Fiske BP, Gui DY, Vander Heiden MG (2015) Lack of evidence for PKM2 protein kinase activity. Mol Cell 59(5):850–857
62. Sizemore ST, Zhang M, Cho JH, Sizemore GM, Hurwitz B, Kaur B, Lehman NL, Ostrowski MC, Robe PA, Miao W et al (2018) Pyruvate kinase M2 regulates homologous recombination-mediated DNA double-strand break repair. Cell Res 28:1090
63. Palsson-McDermott EM, Curtis AM, Goel G, Lauterbach MAR, Sheedy FJ, Gleeson LE, van den Bosch MWM, Quinn SR, Domingo-Fernandez R, Johnston DGW et al (2015) Pyruvate kinase M2 regulates Hif-1alpha activity and IL-1beta induction and is a critical determinant of the warburg effect in LPS-activated macrophages. Cell Metab 21(2):347